



Contents lists available at ScienceDirect

## Radiotherapy and Oncology

journal homepage: www.thegreenjournal.com



## Original article

# High-dose and fractionation effects in stereotactic radiation therapy: Analysis of tumor control data from 2965 patients

Igor Shuryak<sup>a</sup>, David J. Carlson<sup>b,\*</sup>, J. Martin Brown<sup>c</sup>, David J. Brenner<sup>a</sup>

<sup>a</sup> Center for Radiological Research, Columbia University, New York; <sup>b</sup> Department of Therapeutic Radiology, Yale University School of Medicine, New Haven; and <sup>c</sup> Division of Radiation and Cancer Biology, Department of Radiation Oncology, Stanford University, USA

## ARTICLE INFO

## Article history:

Received 31 October 2014

Received in revised form 20 April 2015

Accepted 14 May 2015

Available online xxxx

## Keywords:

Stereotactic  
Radiotherapy  
SBRT  
Model  
Fractionation  
Dose

## ABSTRACT

**Background and purpose:** Two aspects of stereotactic radiotherapy (SRT) require clarification: First, are tumoricidal mechanisms at high-doses/fraction the same as at lower doses? Second, is single high-dose SRT treatment advantageous for tumor control (TCP) vs. multi-fraction SRT?

**Material and methods:** We analyzed published TCP data for lung tumors or brain metastases from 2965 SRT patients, covering a wide range of doses and fraction numbers. We used: (a) a linear-quadratic model (including heterogeneity), which assumes the same mechanisms at all doses, and (b) alternative models with terms describing distinct tumoricidal mechanisms at high doses.

**Results:** Both for lung and brain data, the LQ model provided a significantly better fit over the entire range of treatment doses than did any of the models requiring extra terms at high doses. Analyzing the data as a function of fractionation (1 fraction vs. >1 fraction), there was no significant effect on TCP in the lung data, whereas for brain data multi-fraction SRT was associated with higher TCP than single-fraction treatment.

**Conclusion:** Our analysis suggests that distinct tumoricidal mechanisms do not determine tumor control at high doses/fraction. In addition, there is evidence suggesting that multi-fraction SRT is superior to single-dose SRT.

© 2015 The Authors. Published by Elsevier Ireland Ltd. Radiotherapy and Oncology xxx (2015) xxx–xxx  
This is an open access article under the CC BY-NC-ND license (<http://creativecommons.org/licenses/by-nc-nd/4.0/>).

Stereotactic radiosurgery (SRS) and stereotactic body radiotherapy (SBRT), also known as stereotactic ablative radiotherapy (SABR), are becoming increasingly accepted [1]. The spatial accuracy of dose delivery using these techniques (hereafter referred to as stereotactic radiotherapy, SRT) allows substantial dose escalation to the tumor [1].

Over the past three decades, radiotherapy design has been guided by the linear-quadratic (LQ) model [2–4]. Clinical results, even for some non-standard scenarios (hyperfractionation [5], high- vs. low dose-rate brachytherapy [6], prostate hypofractionation [7]) were consistent with LQ predictions. In contrast to earlier approaches [8–10], there have been no major failures.

Some investigators have argued that tumor eradication by large doses/fraction is dominated by distinct biological phenomena (e.g., damage to the tumor vasculature) that are qualitatively different from those operating at lower doses, and therefore are not accounted for by the LQ model [11–17]. By contrast, others argue [18,19] that SRT effectiveness is sufficiently explained by increased

tumor doses, which destroy tumors largely through the same mechanisms that operate at lower doses.

In this paper, therefore, we address the question as to whether tumoricidal mechanisms at high-doses/fraction are the same as at lower doses – or are there new mechanisms at play specifically at high doses? We approach this question by analyzing a large data set for TCP vs. dose from SRT patients for lung tumors or brain metastases, covering a wide range of doses and fraction numbers. We analyze these data with the LQ model, which assumes the same mechanisms at all doses, and also with alternative models which incorporate extra terms describing different cell killing mechanisms at high doses.

## Materials and methods

### Data sets

Using the PubMed and Google Scholar databases, we searched for articles published in the past 15 years (up to 3/15/2013) that met the following criteria: (1) the reported radiotherapy regimens had to be classified as some form of SRT; (2) TCP had to be reported for  $\geq 1$  year following SRT for brain and/or lung tumors/metastases; (3) the number of fractions, and the dose per fraction had

\* Corresponding author at: Center for Radiological Research, Columbia University, New York, NY 10032, USA.

E-mail address: [djb3@cumc.columbia.edu](mailto:djb3@cumc.columbia.edu) (D.J. Carlson).

<http://dx.doi.org/10.1016/j.radonc.2015.05.013>

0167-8140/© 2015 The Authors. Published by Elsevier Ireland Ltd.

This is an open access article under the CC BY-NC-ND license (<http://creativecommons.org/licenses/by-nc-nd/4.0/>).

to be specified, preferably for more than one radiotherapy regimen; (4) information had to be provided allowing estimation of doses both to the isocenter and to the periphery (generally at least 80% of the prescribed isocenter dose covered the PTV).

We found 33 publications, which together contained data from 2965 patients, mostly treated for early-stage non-small cell lung cancer (NSCLC) or brain metastases. We extracted data on TCP values from 59 treatment regimens (Table 1). For each regimen, we extracted (or estimated, if it was not reported explicitly) the

**Table 1**

Summary of the analyzed data sets. The majority of patients in the brain data set were treated for metastatic brain tumors, and the majority of patients in the lung data set were treated for early stage non-small cell lung cancer.

Published data set	Reference	Cancer site	Mean # of fractions	Mean isocentral dose/fraction (Gy)	# of patients
Chang	[44]	Brain	1.0	23.5	10
Chang	[44]	Brain	1.0	20.0	61
Chang	[45]	Brain	1.0	21.0	130
Chao	[46]	Brain	1.0	20.6	50
Chao	[46]	Brain	1.0	28.8	61
Engenhart	[47]	Brain	1.0	21.5	57
Lutterbach	[48]	Brain	1.0	22.5	101
Matsuo	[49]	Brain	1.0	25.0	30
Matsuo	[49]	Brain	1.0	50.0	30
Molenaar	[50]	Brain	1.0	16.9	29
Molenaar	[50]	Brain	1.0	23.8	29
Molenaar	[50]	Brain	1.0	28.8	28
Shiau	[51]	Brain	1.0	25.0	4
Shiau	[51]	Brain	1.0	33.0	30
Shiau	[51]	Brain	1.0	41.0	66
Shirato	[52]	Brain	1.0	25.0	39
Vogelbaum	[53]	Brain	1.0	30.0	9
Vogelbaum	[53]	Brain	1.0	36.0	12
Vogelbaum	[53]	Brain	1.0	48.0	27
Higuchi	[54]	Brain	3.0	20.0	43
Saitoh	[55]	Brain	3.0	13.0	15
Saitoh	[55]	Brain	3.0	14.0	34
Narayana	[20]	Brain	5.0	6.0	20
Ernst	[56]	Brain	5.0	7.8	22
Fritz	[57]	Lung	1.0	30.0	40
Hof	[58]	Lung	1.0	22.0	10
Hof	[58]	Lung	1.0	28.0	32
Trakul	[59]	Lung	1.0	30.0	48
Crabtree	[60]	Lung	3.0	21.8	76
Fakiris	[61]	Lung	3.0	26.3	70
Grills	[62]	Lung	3.0	22.5	209
Grills	[62]	Lung	3.0	25.0	22
Kopek	[63]	Lung	3.0	15.0	89
Koto	[64]	Lung	3.0	15.0	20
Olsen	[65]	Lung	3.0	21.4	111
Ricardi	[66]	Lung	3.0	18.8	62
Taremi	[67]	Lung	3.0	23.5	29
Taremi	[67]	Lung	3.0	22.5	19
Timmerman	[68]	Lung	3.0	22.5	55
Ng	[69]	Lung	3.2	18.9	20
Chang	[70]	Lung	4.0	15.2	130
Nagata	[71]	Lung	4.0	12.0	45
Shibamoto	[72]	Lung	4.0	11.0	4
Shibamoto	[72]	Lung	4.0	12.0	124
Shibamoto	[72]	Lung	4.0	13.0	52
Shirata	[73]	Lung	4.0	12.0	45
Taremi	[67]	Lung	4.0	15.1	41
Trakul	[59]	Lung	4.0	15.0	60
Grills	[62]	Lung	4.2	15.0	172
Haasbeek	[74]	Lung	4.9	15.5	193
Olsen	[65]	Lung	5.0	10.7	8
Olsen	[65]	Lung	5.0	11.9	11
Takeda	[75]	Lung	5.0	12.5	63
Grills	[62]	Lung	5.1	13.9	102
Koto	[64]	Lung	8.0	7.5	11
Shirata	[73]	Lung	8.0	7.5	29
Taremi	[67]	Lung	8.0	9.6	9
Taremi	[67]	Lung	10.0	5.8	10
Shirata	[73]	Lung	15.0	4.0	7

number of treated patients. The majority of treatment regimens (46 out of 59) were performed using LINAC equipment. There were no 3D-CRT regimens and only one IMRT regimen [20]. Median ages of the treated patients ranged from 52 to 79, with a mean of 67. Maximum tumor diameters ranged from 2.0 to 10.0 cm, with a mean of 5.2 cm.

Thirty-one percent of the patients were treated with single-fraction regimens with a median dose of 19.0 (range: 12.5, 25.0) Gy to the periphery and 25.0 (range: 16.9, 50.0) Gy to the isocenter. The median number of fractions for the fractionated regimens was 4 (range: 3, 15), and the median dose per fraction was 11.4 Gy (range: 3.2, 22.7) to the tumor periphery and 14.5 Gy (range: 4.0, 26.3) to the isocenter. The median TCP was 0.83 (range: 0.16 to 1.0). These values are consistent with previous studies of SRT (e.g., [21,22]). Increasing the minimum acceptable time for reported TCP after SRT from 1 years to 3 years did not change the TCP numbers dramatically (reducing the median TCP to 0.76), but dramatically reduced the number of available publications (from 33 to 15).

### Radiobiological models

Our overall goal here is to investigate whether the SRT tumor control data imply that there are new tumoricidal mechanisms that determine tumor control at high SRT doses – mechanisms which are not present or have little effect at conventional radiotherapeutic doses. To accomplish this, we investigate whether the standard LQ model with heterogeneity can provide as good a description of the SRT data as can models with extra terms describing unique high-dose tumor control mechanisms.

The mechanistically-motivated model most often used to describe radiotherapeutic tumor control is the linear quadratic model [2–7], which has more recently been used to include heterogeneity, within and/or between tumors [23–28]. Consequently, as an example of a model which assumes that the same tumoricidal mechanisms operate at all radiation doses, we used the LQ model with heterogeneous tumor cell radiosensitivity (within a given tumor). Details of the LQ model, and its extension to heterogeneous tumor cell radiosensitivity, are given in Appendix A.

As examples of models which have been developed to describe the proposed and as yet not fully specified distinct tumoricidal mechanisms at high radiation doses, we used the Linear Quadratic Linear (LQL) [29,30], Universal Survival Curve (USC) [31], the Pade Linear Quadratic (PLQ) [32] formalisms (details are given in Appendix A).

It may be noted that models such as LQL, USC and PLQ assume homogeneous tumor sensitivity [29–32], though they are all amenable to extension including heterogeneous radiosensitivity. In the Results section we briefly describe results for heterogeneous versions of these models. However our primary focus here is to assess whether the extra high-dose terms in LQL, USC and PLQ are needed to describe the high dose SRT data, or whether the more established effects of heterogeneity are sufficient.

### Model fitting and comparison procedures

For each radiotherapy regimen, there were  $n$  treated patients, and local tumor control was achieved for  $k$  of them, where  $k = n$  TCP. Each radiobiological model predicted a TCP value ( $p$ ), based on which the binomial log likelihood  $\ln[L(p,n,k)]$  was calculated. Model fitting involved maximizing the sum of  $\ln[L(p,n,k)]$  over all regimens.

Ranking of models by relative goodness of fit, taking into account sample size and parameter number, was based on the Akaike information criterion with sample size correction (AICc), which has gained widespread popularity for this purpose [33,34].

For ranking non-linear models, AICc is preferable to methods that rely on reduced  $X^2$  or  $R^2$  [35–38]. Another useful property of AICc is that more than two models can be compared simultaneously, without the need for models to be “nested” or to belong to the same class. The model which has the lowest AICc value among those being compared is the best-fitting model, and those models which have AICc  $\geq 6$  units higher than the best-fitting model have much poorer support from the data. More details about the use of AICc information criterion are in Appendix B. Confidence intervals for best-fit model parameter values were estimated by profile likelihood [39].

The relative importance of heterogeneous (HET) tumor cell radiosensitivity, compared with extra parameters which modify the cellular dose response shape at high doses, was calculated by the ratio  $R = W_{\text{HET}}/W_{\text{noHET}}$ , where  $W_{\text{HET}}$  is the sum of Akaike weights (described in Appendix B) for the heterogeneous LQL, PLQ, and USC models fitted to the same data, and  $W_{\text{noHET}}$  is the corresponding sum of Akaike weights for the homogeneous versions of the same models.

## Results

Visual inspection of best-fit predictions from the analyzed models (Figs. 1 and 2) suggests that the LQ model with heterogeneous radiosensitivity provides a much better description of the SRT TCP data as compared with the models (LQL, PLQ and USC) which include an extra high-dose mechanism. Statistical analysis support for this difference in fit quality (by AICc, which accounts for model complexity as well as closeness of the fit to the data) is overwhelming both for the lung and for the brain data (Table 2): The LQL, PLQ and USC formalisms have AICc values which are hundreds of units higher than the heterogeneous LQ model, suggesting that these formalisms have effectively no support from the data,

compared with the LQ model. In essence, given a biologically plausible initial number ( $N$ ) of clonogenic tumor cells of  $10^5$ , the LQL, PLQ and USC produced TCP dose responses which were too steep to describe the data well (Figs. 1 and 2). At larger values of  $N$  this effect became even stronger (not shown). Using this same initial number of clonogenic tumor cells ( $10^5$ ), the LQ model with heterogeneity predicts a much shallower dose response, thereby bringing the model predictions much closer to the data. These results remained qualitatively unchanged regardless of whether we used doses to the isocenter (Figs. 1 and 2, Table 2), or to the periphery (not shown). They were also robust in response to altered assumptions about the  $\alpha/\beta$  ratio: for example, when the ratio was increased from 10 Gy to 20 Gy, or was allowed to become freely adjustable.

The model comparison suggests that the addition of extra high-dose modification terms (implemented in LQL, USC, and PLQ models) had much less effect on model performance, than the inclusion of heterogeneous radiosensitivity, which dramatically improved agreement with SRT data for all models (Table 2, Figs. 1 and 2). The relative importance ( $R$ ) of heterogeneous tumor cell radiosensitivity, compared with extra parameters which modify the cellular dose response shape at high doses, was quantified for the LQL, PLQ and USC as described in Materials and Methods. For the lung single-fraction data,  $R \geq 98.7$ , and  $R$  was effectively infinite ( $>10^9$ ) for all other data subsets. In other words, accounting for variability in radiosensitivity is more important for describing the TCP data, than adjusting the details of cell survival curve shape at high doses.

To assess the effects of SRT fractionation on predicted TCP, single-fraction and multiple-fraction regimens were fitted separately. Using the best-fitting LQ model, for lung tumors fractionation effects could not be detected with confidence – when the model was fitted to single-fraction and multiple-fraction data

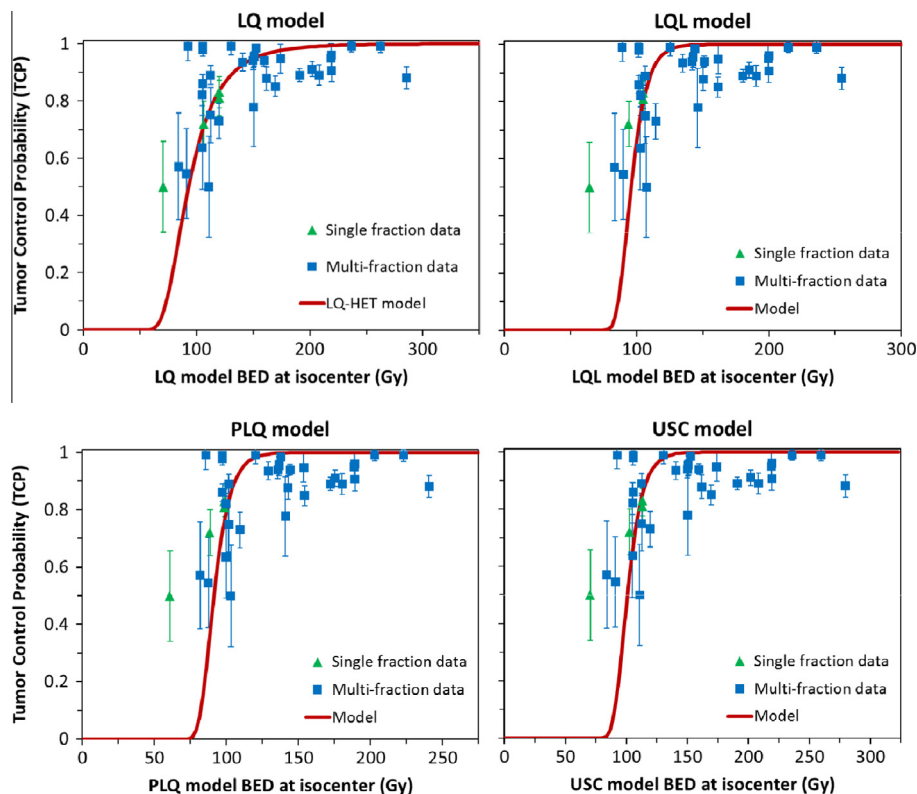


**Fig. 1.** Best fits to data on early-stage NSCLC from the LQ model with heterogeneous radiosensitivity (LQ), and from the LQL, PLQ and USC models with homogeneous radiosensitivity. In this and the following figures, error bars represent standard errors.

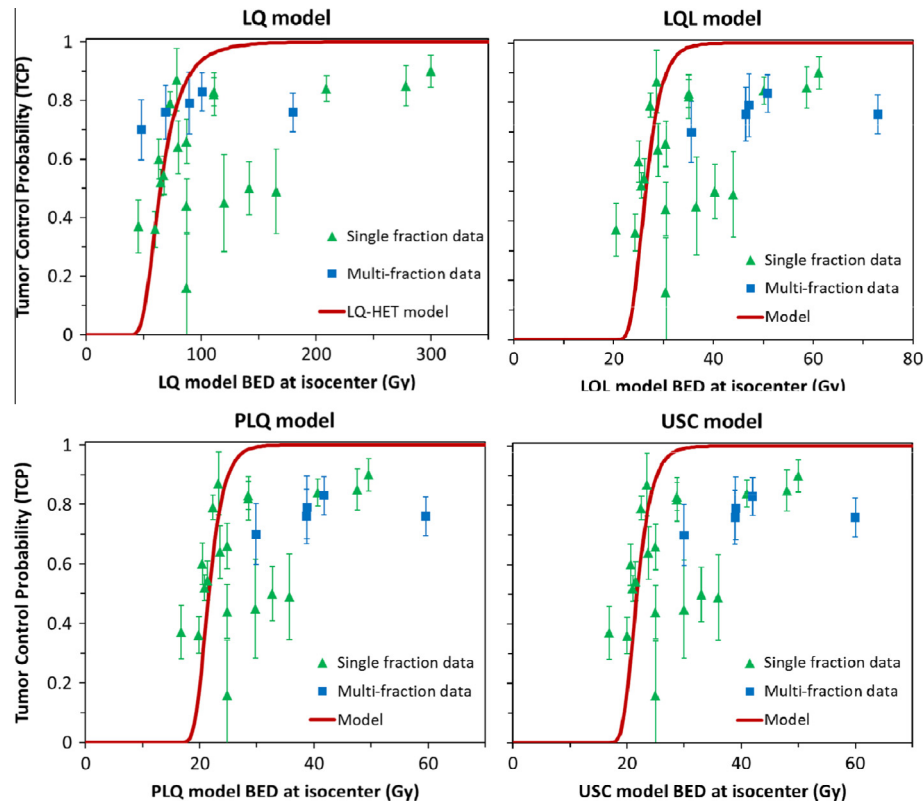


**Fig. 2.** Best fits to data on brain metastases from the LQ model with heterogeneous radiosensitivity (LQ), and from the LQL, PLQ and USC models with homogeneous radiosensitivity.

**Table 2**  
Best-fit parameter values and relative fit quality assessment (by  $\Delta\text{AICc}$ ) for the LQ model with heterogeneous radiosensitivity (LQ), and for the LQL, PLQ and USC models with homogeneous radiosensitivity. Doses to the isocenter were used. The symbol  $p_1$  refers to the extra parameter (compared with the LQ model) which is present in the LQL, PLQ and USC models (but has a different meaning and different units in each model, described in Appendix A).  $\Delta\text{AICc}$  is the result of an information-theoretic analysis for comparing fit quality for different models on the same data.  $\Delta\text{AICc} = 0$  for the best-fitting model, and models with large  $\Delta\text{AICc}$  values ( $>6$ ) have much poorer support from the data. Details are discussed in the main text and in Appendix B.

Fraction #	Cancer site	Model	$\alpha$ ( $\text{Gy}^{-1}$ , 95% CI)			$p_1$ (95% CI)			$\Delta\text{AICc}$
All	Lung	LQ	0.12	0.12	0.13	0.019	0.016	0.022	1664.4
All	Lung	PLQ	0.13	0.13	0.13	0.007	0.006	0.008	1661.6
All	Lung	USC	0.12	0.12	0.12	1.58	1.40	1.66	1607.7
All	Lung	LQ	0.40	0.39	0.42	–	–	–	0
1	Lung	LQL	0.47	0.45	0.48	$\infty$	$\infty$	$\infty$	21.7
1	Lung	PLQ	47.81	46.43	49.27	14.11	13.69	14.52	0
1	Lung	USC	0.47	0.30	0.73	2.14	2.07	2.21	21.7
1	Lung	LQ	0.43	0.40	0.46	–	–	–	1.1
>1	Lung	LQL	0.26	0.25	0.26	$\infty$	$\infty$	$\infty$	552
>1	Lung	PLQ	0.42	0.41	0.42	0.210	0.207	0.214	510.9
>1	Lung	USC	0.26	0.21	0.32	3.92	3.88	3.96	552
>1	Lung	LQ	0.40	0.39	0.41	–	–	–	0
All	Brain	LQL	0.45	0.45	0.45	0.873	0.841	0.913	991.4
All	Brain	PLQ	0.55	0.55	0.56	0.101	0.099	0.103	986.1
All	Brain	USC	0.55	0.45	0.64	1.83	1.82	1.84	987.1
All	Brain	LQ	0.58	0.57	0.59	–	–	–	0
1	Brain	LQL	0.56	0.55	0.56	$\infty$	$\infty$	$\infty$	484.4
1	Brain	PLQ	15.85	15.69	16.01	4.16	4.12	4.20	67.7
1	Brain	USC	0.56	0.48	0.64	1.80	1.78	1.81	484.3
1	Brain	LQ	0.57	0.55	0.58	–	–	–	0
>1	Brain	LQL	0.35	0.34	0.37	$\infty$	$\infty$	$\infty$	148.1
>1	Brain	PLQ	4.29	4.17	4.41	2.47	4.39	2.54	0
>1	Brain	USC	0.35	0.31	0.41	2.83	2.75	2.90	148.1
>1	Brain	LQ	0.66	0.62	0.72	–	–	–	65.9

separately, the 95% CIs for  $\alpha$  overlapped (Table 2). However, for brain metastases the evidence from the data suggested that multi-fraction SRT regimens had higher effectiveness than single-fraction regimens (see  $\alpha$  values and non-overlapping 95% CIs in Table 2, and curves in Fig. 3).

If the  $\alpha/\beta$  ratio was increased from 10 Gy to 20 Gy and/or if peripheral doses were used, the evidence became too weak to differentiate between best-fit  $\alpha$  values for single vs multiple-fraction SRT. For example, using isocenter doses and an  $\alpha/\beta$  ratio of 20 Gy, the best-fit LQ  $\alpha$  value for single-fraction SRT was 0.857 (95% CI:

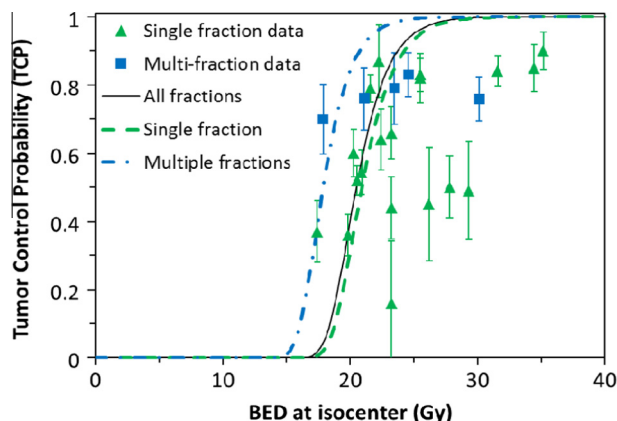


Fig. 3. Best fits of the LQ model with heterogeneous radiosensitivity to data on brain metastases treated with single-fraction vs. multiple-fraction SRT.

0.837, 0.877), and for multi-fraction SRT it was 0.834 (95% CI: 0.781, 0.898). Consequently, regardless of the  $\alpha/\beta$  ratio, there was no support for the hypothesis that single-fraction regimens are inherently more effective than multiple fractions [14–17], and at a biologically plausible  $\alpha/\beta$  ratio of 10 Gy there was some support for higher effectiveness of *multiple* fractions.

## Discussion

The LQ model with heterogeneous radiosensitivity, which assumes that the same tumoricidal mechanisms operate at all doses and fraction numbers, provided a much better description of the SRT tumor control data over the entire dose range than did any of the models which assumed unique extra tumoricidal mechanism at high doses. These results, therefore, along with similarly motivated analyses [18,19,40], do not support the argument [11–17] that tumor response to high-dose SRT is fundamentally different from that which would be predicted from responses at conventional dose fractionations.

For example, proposed high-dose-specific tumoricidal mechanisms such as damage to the tumor vasculature [11–17] should enhance the TCP at high doses/fraction, predicting a steep dose response for TCP. The data, by contrast, support a shallow dose response which is reasonably explained by heterogeneity in radiosensitivity (and perhaps heterogeneity in other factors, such as spatial dose distribution [25–27]).

First, we conclude that because the formalisms which attempt to describe the tumor dose response at SRT doses by explicitly accounting for unique high-dose-specific tumoricidal mechanisms fit the data much worse than the heterogeneous LQ formalism which assumes the same mechanisms at all doses, there is no evidence from SRT tumor control data that the proposed high-dose-specific mechanisms dominate tumor control at high doses and/or at small fraction numbers. Rather, the effects of heterogeneous radiosensitivity dominate the comparatively subtle differences between the dose–response shapes produced by different radiobiological models [41]. In short, even if there are unique tumoricidal mechanisms at play at high doses, they are not the major determinants of tumor control by SRT.

Second, based on analyzing the data with the heterogeneous LQ model (including heterogeneity), there was no evidence that single-fraction SRT produces better tumor control than multi-fraction regimens. Instead, multi-fraction brain SRT was predicted to produce slightly better TCPs than single-fraction treatments for brain metastases. These conclusions are consistent with expected effects on hypoxic tumors, where fractionation allows tumor reoxygenation between fractions [41–43].

The strengths of our study include: (1) use of large amount of clinical data (from 2965 SRT-treated patients); (2) use of multiple radiobiological models, some of which (LQ) assume that the same tumoricidal mechanisms determine TCP at all doses and fraction numbers, whereas others (LQL, USC, PLQ) explicitly account for potential high-dose-specific tumoricidal mechanisms; and (3) use of a robust criterion (AICc) to compare support from the data for each of these models [33,34]. The main weaknesses (which are inherent in most similar analyses) involve: (1) fitting summary data vs. individual-patient data; and (2) oversimplification of tumor radiation response by not accounting for effects of tumor size and stage, time after SRT when TCP was reported, patient age and sex, calendar year and institution-specific factors, and many other potential effects. However, because these weaknesses are the same for all considered models, relative comparison of model fit quality can provide insights into how well (or how poorly) does each model capture the main features of tumor response to SRT.

In summary, the TCP data from modern SRT can be reasonably described by models which assume that the same tumoricidal mechanisms determine TCP at all doses and fraction numbers. Consequently, the use of such models remains a clinically successful and mechanistically plausible approach for guiding radiotherapy design.

## Conflict of interest

None.

## Appendix A

### A.1. Radiobiological models

#### A.1.1. Linear quadratic (LQ) model

The LQ model is a mechanistic consequence of repair/misrepair kinetics of radiation-induced DNA double strand breaks (DSBs) [76,77]. Differences in fractionation response between tissues [78] are quantified through differences in the ratio of parameters  $\alpha$  and  $\beta$ , and this ratio (here labeled as  $r = \alpha/\beta$  for convenience) can be directly derived from clinical data.

The LQ formalism postulates that the fraction of cells which survive an acute radiation dose  $d$  is determined by the following expression [79,80].

$$S_{lq} = \exp[-\alpha d - \alpha/r d^2] \quad (A1)$$

For simplicity, we assume that the heterogeneity in tumor cell radiosensitivity applies to the linear term ( $\alpha$ ) of the LQ model, because this term was shown to be most influential numerically [23,25,81]. Mathematically, this is implemented as follows.

We introduce a dummy variable  $a$ , which is randomly distributed, from zero to infinity, according to the Gamma distribution, with a mean value of  $\alpha$  and a shape parameter  $g$  (restricted to integers  $\geq 2$  for convenience). The Gamma distribution was selected instead of the Gaussian distribution because, consistently with biological plausibility, it converges to zero at  $\alpha = 0$  (whereas the Gaussian distribution does not), and generates a simple analytic solution for TCP for several tested models (see below).

The probability density function (PDF) is:

$$PDF = a^g \exp[-(g+1)a/\alpha] / (g+1)^{(g+1)} / (\alpha^{(g+1)} g!) \quad (A2)$$

The clonogenic survival probability ( $S_{het}$ ) for the heterogeneous population of tumor cells exposed to a radiotherapy regimen composed of  $m$  acute dose fractions with  $d$  Gy per fraction (and assuming sufficient time for complete DNA damage repair between fractions) is calculated as follows:

$$S_{het} = \int_0^{\infty} PDF S_{iq} da = \exp[(g+1)\ln(g+1)]r^{(g+1)}/(\alpha m d(d+1) + r(g+1))^{(g+1)} \quad (A3)$$

Alternatively,  $S_{het}$  can also be expressed as function of BED calculated using the LQ model:

$$S_{het} = (g+1)^{(g+1)}/(\alpha BED + g+1)^{(g+1)} \quad (A4)$$

We assume that tumor control occurs when all tumor clonogens (i.e., cells capable of repopulating the tumor) have been killed, and that the number of such clonogens at the end of radiotherapy is Poisson distributed with a mean of  $N S_{het}$ , where  $N$  is the number of clonogens before treatment. The predicted TCP for the LQ model with heterogeneity is then given by the following expression:

$$TCP_{het} = \exp[-N S_{het}] \quad (A5)$$

#### A.1.2. Linear quadratic linear (LQL) model

The Linear Quadratic Linear (LQL) [29,30] model was developed to modify the LQ model through the replacement of the continuously bending terminal part of the dose response curve for the logarithm of cell survival by the corresponding exponential cell inactivation mode. This was accomplished by modification of the “G-factor” which represents damage repair between radiation dose fractions. The resulting equation for the average number of lethal events per cell is as follows, where  $\alpha$ ,  $r$  and  $p_1$  are adjustable parameters:

$$\alpha d + 2\alpha/r(p_1 d - 1 + \exp[-p_1 d])/p_1^2 \quad (A6)$$

#### A.1.3. Universal survival curve (USC) model

In the USC model, the transition from curved to straight dose response for the logarithm of cell survival is done by introducing a cut-off or transition dose by means of the discontinuous, Heaviside step function. The resulting equation for the average number of lethal events per cell is:

$$\alpha d + \alpha d^2/r \text{ for } d \leq r(1 - \alpha p_1)/(2\alpha p_1), \text{ and} \\ d/p_1 - r(1 - \alpha p_1)^2/(4\alpha p_1^2) \text{ for } d > r(1 - \alpha p_1)/(2\alpha p_1) \quad (A7)$$

#### A.1.4. Pade linear quadratic (PLQ) model

In the PLQ model, the dose response shape is gradually altered, becoming less curved at high doses, by the presence of a term  $1 + p_1 d$  in the denominator of the function for the average number of lethal events per cell is:

$$(\alpha d + \alpha d^2/r)/(1 + p_1 d) \quad (A8)$$

#### A.1.5. Model parameters

Exploratory calculations using the LQ model with heterogeneous tumor cell radiosensitivity showed that increasing the initial number of tumor clonogenic cells ( $N$ ) and/or decreasing the  $\alpha/\beta$  ratio ( $r$ ) generally decreased fit quality (increased the Akaike information criterion with sample size correction (AICc) [33,34]). Consequently, low values of  $N$  and high (effectively infinite) values of  $r$  were preferred in unrestricted fits, but sensitivity to these parameters was much lower than to  $\alpha$ . To maintain biological plausibility and simplify the model, we restricted  $r$  to 10 Gy and  $N$  to  $10^5$  clonogens.

Eqs. (A6)–(A8) were used to calculate TCP for the LQL, PLQ and USC models in the same manner as described for the LQ model in Eq. (A5). Mathematically, this involved replacing the LQ model-based cell killing term  $L_F = (\alpha d + \alpha r d^2)$  from Eq. (A1) with the corresponding term from the alternative model, where  $p_1$  is an additional adjustable parameter (with different meaning and

different units in each model). We applied the same parameter restrictions to these models as to the LQ model described above.

In the heterogeneous versions of each model, the shape parameter  $g$  for the Gamma probability distribution of  $\alpha$  values is an additional adjustable parameter. Values of  $2 < g < 6$  were preferred in unrestricted exploratory fits, but sensitivity to  $g$  in this range was much lower than to  $\alpha$ . To maintain biological plausibility for the width of the distribution of  $\alpha$  values, we restricted  $g$  to 5. The resulting distribution approximates a “bell-shaped” curve.

The only remaining parameter in the heterogeneous LQ model was therefore  $\alpha$ , which could be interpreted as a measure of tumor radiosensitivity. We followed the same rationale for restricting parameters in alternative radiobiological models. The LQL, USC, and PLQ models each contain parameters analogous to  $\beta$  or to  $\alpha/\beta$  from the LQ model. We restricted these analogous parameters to correspond to the condition  $r = 10$  Gy. Parameter  $N$  was set to  $10^5$  for all models.

Consequently, the homogenous LQL, USC, and PLQ models each contained two adjustable parameters:  $\alpha$  and a model-specific high-dose modification term ( $p_1$ ). Heterogeneous versions of these models contained an extra parameter ( $g$ ). Thus, for the purposes of calculating AICc scores, the total number of adjustable parameters was 2 for the LQL, PLQ, USC, and heterogeneous LQ models, and 3 for the heterogeneous LQL, PLQ, and USC models.

Exploratory calculations showed that the best fits (lowest AICc values) for all models to lung data were produced using isocentral SRT doses. For brain data the trend was reversed: peripheral doses produced better fits, but the difference in fits using peripheral or isocentral doses was not as great as for the lung. Consequently, we selected isocentral doses as the default for our analysis for both lung and brain data. The main conclusions (described below) were not changed if peripheral doses were used.

#### A.1.6. Exploration of heterogeneity using alternative models

An analytic solution was produced for the heterogeneous PLQ model, along the same lines as for the LQ model described above. For the heterogeneous LQL and USC models, numerical integration was necessary. In addition, we performed exploratory calculations using the same models, but assuming that the heterogeneity applies to radiosensitivity of tumors in different patients, rather than to the radiosensitivity of tumor cells within a patient. For this inter-tumor heterogeneity scenario, one exponentiation is carried inside the integral, which leads to the following equation:

$$TCP_{het(inter)} = \int_0^{\infty} PDF e^{-N S_{het}} da \quad (A9)$$

Eq. (A9) has no analytic solution and needed to be evaluated numerically for all models

## Appendix B

### B.1. Use of the akaike information criterion with correction for sample size (AICc)

AICc is rooted in information theory, and assesses how much Kullback–Leibler information is lost when each tested model is used to approximate the data. The model that loses the least amount of information relative to other compared models is considered the best. The equation for AICc is below, where LL is the log likelihood (the maximized value, produced by best-fit parameter values),  $q$  is the number of model parameters, and  $N_s$  is sample size (number of patients):

$$AICc = -2LL + 2q + 2q(q+1)/(N_s - q - 1) \quad (B10)$$

One of the most convenient features of using AICc is that it allows the evidence for multiple structurally distinct models to be compared. For example, consider  $i = 1 \dots n$  compared models. The relative likelihood of the ( $i$ th) model, called the evidence ratio ( $E_{r(i)}$ ), can be expressed as:

$$E_r(i) = \exp[-\Delta\text{AICc}_{(i)}/2], \text{ where } \Delta\text{AICc}_{(i)} = \text{AICc}_{(i)} - \text{AICc}_{(\min)} \quad (\text{B11})$$

Here  $\text{AICc}_{\min}$  is the lowest AICc value generated by the set of  $n$  models being compared. If  $\Delta\text{AICc}_{(i)} > 6$ , then the evidence ratio  $E_{r(i)} < 0.05$ , suggesting that the tested model has poor support from the data relative to the best-fitting model in the set of models being compared.

The Akaike weight,  $w_{(i)}$ , is another useful quantity – it represents the probability that the tested model would be considered the best-fitting model upon repeated sampling of the data. It is a normalized evidence ratio, i.e. the evidence ratio for the tested model divided by the sum of the evidence ratios for all the models being compared:

$$w_{(i)} = E_{r(i)} / \sum_{i=1}^n E_{r(i)} \quad (\text{B12})$$

## References

- [1] Hadziahmetovic M, Loo BW, Timmerman RD, et al. Stereotactic body radiation therapy (stereotactic ablative radiotherapy) for stage I non-small cell lung cancer—updates of radiobiology, techniques, and clinical outcomes. *Discov Med* 2010;9:411–7.
- [2] Miralbell R, Roberts SA, Zubizarreta E, Hendry JH. Dose-fractionation sensitivity of prostate cancer deduced from radiotherapy outcomes of 5,969 patients in seven international institutional datasets:  $\alpha/\beta = 1.4$  (0.9–2.2) Gy. *Int J Radiat Oncol Biol Phys* 2012;82:e17–24.
- [3] Livi L, Buonamici FB, Simontacchi G, et al. Accelerated partial breast irradiation with IMRT: new technical approach and interim analysis of acute toxicity in a phase III randomized clinical trial. *Int J Radiat Oncol Biol Phys* 2010;77:509–15.
- [4] Owen JR, Ashton A, Bliss JM, et al. Effect of radiotherapy fraction size on tumour control in patients with early-stage breast cancer after local tumour excision: long-term results of a randomised trial. *Lancet oncol* 2006;7:467–71.
- [5] Leborgne F, Leborgne JH, Fowler J, Zubizarreta E, Mezzera J. Accelerated hyperfractionated irradiation for advanced head and neck cancer: effect of shortening the median treatment duration by 13 days. *Head Neck* 2001;23:661–8.
- [6] Brenner DJ, Hall EJ. Fractionation and protraction for radiotherapy of prostate carcinoma. *Int J Radiat Oncol Biol Phys* 1999;43:1095–101.
- [7] Yeoh EE, Botten RJ, Butters J, et al. Hypofractionated versus conventionally fractionated radiotherapy for prostate carcinoma: final results of phase III randomized trial. *Int J Radiat Oncol Biol Phys* 2011;81:1271–8.
- [8] Brenner DJ. The linear-quadratic model is an appropriate methodology for determining isoeffective doses at large doses per fraction. *Semin Radiat Oncol* 2008;18:234–9.
- [9] Kirkpatrick JP, Brenner DJ, Orton CG. Point/Counterpoint. The linear-quadratic model is inappropriate to model high dose per fraction effects in radiosurgery. *Med Phys* 2009;36:3381–4.
- [10] Brenner DJ, Sachs RK, Peters LJ, Withers HR, Hall EJ. We forget at our peril the lessons built into the alpha/beta model. *Int J Radiat Oncol Biol Phys* 2012;82:1312–4.
- [11] Kirkpatrick JP, Meyer JJ, Marks LB. The linear-quadratic model is inappropriate to model high dose per fraction effects in radiosurgery. *Semin Radiat Oncol* 2008;18:240–3.
- [12] Kocher M, Treuer H, Voges J, et al. Computer simulation of cytotoxic and vascular effects of radiosurgery in solid and necrotic brain metastases. *Radiation Oncol* 2000;54:149–56.
- [13] Yamada Y, Bilsky MH, Lovelock DM, et al. High-dose, single-fraction image-guided intensity-modulated radiotherapy for metastatic spinal lesions. *Int J Radiat Oncol Biol Phys* 2008;71:484–90.
- [14] Fuks Z, Kolesnick R. Engaging the vascular component of the tumor response. *Cancer cell* 2005;8:89–91.
- [15] Park HJ, Griffin RJ, Hui S, Levitt SH, Song CW. Radiation-induced vascular damage in tumors: implications of vascular damage in ablative hypofractionated radiotherapy (SBRT and SRS). *Radiat Res* 2012;177:311–27.
- [16] Oermann EK, Kress MA, Todd JV, et al. The impact of radiosurgery fractionation and tumor radiobiology on the local control of brain metastases. *J Neurosurg* 2013;119:1131–8.
- [17] Lippitz B, Lindquist C, Paddick I, et al. Stereotactic radiosurgery in the treatment of brain metastases: the current evidence. *Cancer Treat Rev* 2014;40:48–59.
- [18] Brown JM, Brenner DJ, Carlson DJ. Dose escalation, not “new biology”, can account for the efficacy of stereotactic body radiation therapy with non-small cell lung cancer. *Int J Radiat Oncol Biol Phys* 2013;85:1159–60.
- [19] Brown JM, Carlson DJ, Brenner DJ. The tumor radiobiology of SRS and SBRT: are more than the 5 RS involved? *Int J Radiat Oncol Biol Phys* 2014;88:254–62.
- [20] Narayana A, Chang J, Yenice K, et al. Hypofractionated stereotactic radiotherapy using intensity-modulated radiotherapy in patients with one or two brain metastases. *Stereotact Funct Neurosurg* 2007;85:82–7.
- [21] Matsuyama T, Kogo K, Oya N. Clinical outcomes of biological effective dose-based fractionated stereotactic radiation therapy for metastatic brain tumors from non-small cell lung cancer. *Int J Radiat Oncol Biol Phys* 2013;85:984–90.
- [22] Wiggeraad R, Verbeek-de Kanter A, Kal HB, et al. Dose-effect relation in stereotactic radiotherapy for brain metastases: a systematic review. *Radiation Oncol* 2011;98:292–7.
- [23] Carlone MC, Warkentin B, Stavrev P, Fallone BG. Fundamental form of a population TCP model in the limit of large heterogeneity. *Med Phys* 2006;33:1634–42.
- [24] Schinkel C, Carlone M, Warkentin B, Fallone BG. Analytic investigation into effect of population heterogeneity on parameter ratio estimates. *Int J Radiat Oncol Biol Phys* 2007;69:1323–30.
- [25] Roberts SA, Hendry JH. A realistic closed-form radiobiological model of clinical tumor-control data incorporating intertumor heterogeneity. *Int J Radiat Oncol Biol Phys* 1998;41:689–99.
- [26] Agren Cronqvist AK, Kallman P, Turesson I, Brahma A. Volume and heterogeneity dependence of the dose–response relationship for head and neck tumours. *Acta Oncol* 1995;34:851–60.
- [27] Suit H, Skates S, Taghian A, Okunieff P, Efrid JT. Clinical implications of heterogeneity of tumor response to radiation therapy. *Radiation Oncol* 1992;25:251–60.
- [28] Harting C, Peschke P, Karger CP. Computer simulation of tumour control probabilities after irradiation for varying intrinsic radio-sensitivity using a single cell based model. *Acta Oncol* 2010;49:1354–62.
- [29] Guerrero M, Li XA. Extending the linear-quadratic model for large fraction doses pertinent to stereotactic radiotherapy. *Phys Med Biol* 2004;49:4825–35.
- [30] Guerrero M, Carlone M. Mechanistic formulation of a linear-quadratic-linear (LQL) model: split-dose experiments and exponentially decaying sources. *Med Phys* 2010;37:4173–81.
- [31] Park C, Papiez L, Zhang S, Story M, Timmerman RD. Universal survival curve and single fraction equivalent dose: useful tools in understanding potency of ablative radiotherapy. *Int J Radiat Oncol Biol Phys* 2008;70:847–52.
- [32] Belkic D. Parametric analysis of time signals and spectra from perspectives of quantum physics and chemistry. *Adv Quant Chem* 2011;61:145–260.
- [33] Burnham KP, Anderson DR, Huyvaert KP. AIC model selection and multimodel inference in behavioral ecology: some background, observations, and comparisons. *Behav Ecol Sociobiol* 2011;65:23–35.
- [34] Burnham KP, Anderson DR. Model selection and multi-model inference. a practical information-theoretic approach. Springer; 2002.
- [35] Andrae R, Schulze-Hartung T, Melchior P. Dos and don'ts of reduced chi-squared. arXiv preprint arXiv:10123754 2010.
- [36] Spiess A-N, Neumeyer N. An evaluation of R2 as an inadequate measure for nonlinear models in pharmacological and biochemical research: a Monte Carlo approach. *BMC Pharmacol* 2010;10:6.
- [37] Bentler PM. Comparative fit indexes in structural models. *Psychol Bull* 1990;107:238.
- [38] McQuarrie ADR, Tsai C-L. Regression and time series model selection. Singapore, River Edge, N.J.: World Scientific; 1998.
- [39] Venzon D, Moolgavkar S. A method for computing profile-likelihood-based confidence intervals. *Appl Stat* 1988;87–94.
- [40] Guckenberger M, Klement RJ, Allgauer M, et al. Applicability of the linear-quadratic formalism for modeling local tumor control probability in high dose per fraction stereotactic body radiotherapy for early stage non-small cell lung cancer. *Radiation Oncol* 2013;109:13–20.
- [41] Lindblom E, Dasu A, Lax I, Toma-Dasu I. Survival and tumour control probability in tumours with heterogeneous oxygenation: a comparison between the linear-quadratic and the universal survival curve models for high doses. *Acta Oncol* 2014;53:1035–40.
- [42] Carlson DJ, Keall PJ, Loo Jr BW, Chen ZJ, Brown JM. Hypofractionation results in reduced tumor cell kill compared to conventional fractionation for tumors with regions of hypoxia. *Int J Radiat Oncol Biol Phys* 2011;79:1188–95.
- [43] Lindblom E, Antonovic L, Dasu A, et al. Treatment fractionation for stereotactic radiotherapy of lung tumours: a modelling study of the influence of chronic and acute hypoxia on tumour control probability. *Radiat Oncol* 2014;9:149.
- [44] Chang EL, Hassenbusch SJ, Shiu AS. The role of tumor size in the radiosurgical management of patients with ambiguous brain metastases. *Neurosurgery* 2003;53:272–80 (discussion 80–1).
- [45] Chang EL, Seleck U, Hassenbusch 3rd SJ. Outcome variation among “radioresistant” brain metastases treated with stereotactic radiosurgery. *Neurosurgery* 2005;56:936–45 (discussion 936–45).
- [46] Chao ST, Barnett GH, Vogelbaum et al. Salvage stereotactic radiosurgery effectively treats recurrences from whole-brain radiation therapy. *Cancer* 2008;113:2198–204.

- [47] Engenhardt R, Kimmig BN, Hover KH, et al. Long-term follow-up for brain metastases treated by percutaneous stereotactic single high-dose irradiation. *Cancer* 1993;71:1353–61.
- [48] Lutterbach J, Cyron D, Henne K, Ostertag CB. Radiosurgery followed by planned observation in patients with one to three brain metastases. *Neurosurgery* 2008;62:776–84.
- [49] Matsuo T, Shibata S, Yasunaga A, et al. Dose optimization and indication of Linac radiosurgery for brain metastases. *Int J Radiat Oncol Biol Phys* 1999;45:931–9.
- [50] Molenaar R, Wiggeraad R, Verbeek-de Kanter A, Walchenbach R, Vecht C. Relationship between volume, dose and local control in stereotactic radiosurgery of brain metastasis. *Br J Neurosurg* 2009;23:170–8.
- [51] Shiau CY, Sneed PK, Shu HK, et al. Radiosurgery for brain metastases: relationship of dose and pattern of enhancement to local control. *Int J Radiat Oncol Biol Phys* 1997;37:375–83.
- [52] Shirato H, Takamura A, Tomita M, et al. Stereotactic irradiation without whole-brain irradiation for single brain metastasis. *Int J Radiat Oncol Biol Phys* 1997;37:385–91.
- [53] Vogelbaum MA, Angelov L, Lee SY, et al. Local control of brain metastases by stereotactic radiosurgery in relation to dose to the tumor margin. *J Neurosurg* 2006;104:907–12.
- [54] Higuchi Y, Serizawa T, Nagano O, et al. Three-staged stereotactic radiotherapy without whole brain irradiation for large metastatic brain tumors. *Int J Radiat Oncol Biol Phys* 2009;74:1543–8.
- [55] Saitoh J, Saito Y, Kazumoto T, et al. Therapeutic effect of linac-based stereotactic radiotherapy with a micro-multileaf collimator for the treatment of patients with brain metastases from lung cancer. *Jpn J Clin Oncol* 2010;40:119–24.
- [56] Ernst-Stecken A, Ganslandt O, Lambrecht U, Sauer R, Grabenbauer G. Phase II trial of hypofractionated stereotactic radiotherapy for brain metastases: results and toxicity. *Radiother Oncol* 2006;81:18–24.
- [57] Fritz P, Kraus HJ, Blaschke T, et al. Stereotactic, high single-dose irradiation of stage I non-small cell lung cancer (NSCLC) using four-dimensional CT scans for treatment planning. *Lung Cancer* 2008;60:193–9.
- [58] Hof H, Muentner M, Oetzel D, et al. Stereotactic single-dose radiotherapy (radiosurgery) of early stage nonsmall-cell lung cancer (NSCLC). *Cancer* 2007;110:148–55.
- [59] Trakul N, Chang CN, Harris J, et al. Tumor volume-adapted dosing in stereotactic ablative radiotherapy of lung tumors. *Int J Radiat Oncol Biol Phys* 2012;84:231–7.
- [60] Crabtree TD, Denlinger CE, Meyers BF, et al. Stereotactic body radiation therapy versus surgical resection for stage I non-small cell lung cancer. *J Thorac Cardiovasc Surg* 2010;140:377–86.
- [61] Fakiris AJ, McGarry RC, Yiannoutsos CT, et al. Stereotactic body radiation therapy for early-stage non-small-cell lung carcinoma: four-year results of a prospective phase II study. *Int J Radiat Oncol Biol Phys* 2009;75:677–82.
- [62] Grills IS, Hope AJ, Guckenberger M, et al. A collaborative analysis of stereotactic lung radiotherapy outcomes for early-stage non-small-cell lung cancer using daily online cone-beam computed tomography image-guided radiotherapy. *J Thorac Oncol* 2012;7:1382–93.
- [63] Kopeck N, Paludan M, Petersen J, Grau C, Høyer M. Stereotactic body radiotherapy for medically inoperable stage I non-small cell lung cancer: mature outcome and toxicity results. *Int J Radiat Oncol Biol Phys* 2008;72:537.
- [64] Koto M, Takai Y, Ogawa Y, et al. A phase II study on stereotactic body radiotherapy for stage I non-small cell lung cancer. *Radiother Oncol* 2007;85:429–34.
- [65] Olsen JR, Robinson CG, El Naqa I, et al. Dose-response for stereotactic body radiotherapy in early-stage non-small-cell lung cancer. *Int J Radiat Oncol Biol Phys* 2011;81:e299–303.
- [66] Ricardi U, Filippi AR, Guarneri A, et al. Stereotactic body radiation therapy for early stage non-small cell lung cancer: results of a prospective trial. *Lung Cancer* 2010;68:72–7.
- [67] Taremi M, Hope A, Dafele M, et al. Stereotactic body radiotherapy for medically inoperable lung cancer: prospective, single-center study of 108 consecutive patients. *Int J Radiat Oncol Biol Phys* 2012;82:967–73.
- [68] Timmerman R, Paulus R, Galvin J, et al. Stereotactic body radiation therapy for inoperable early stage lung cancer. *JAMA* 2010;303:1070–6.
- [69] Ng AW, Tung SY, Wong VY. Hypofractionated stereotactic radiotherapy for medically inoperable stage I non-small cell lung cancer—report on clinical outcome and dose to critical organs. *Radiother Oncol* 2008;87:24–8.
- [70] Chang JY, Liu H, Balter P, et al. Clinical outcome and predictors of survival and pneumonitis after stereotactic ablative radiotherapy for stage I non-small cell lung cancer. *Radiat Oncol* 2012;7:152.
- [71] Nagata Y, Takayama K, Matsuo Y, et al. Clinical outcomes of a phase I/II study of 48 Gy of stereotactic body radiotherapy in 4 fractions for primary lung cancer using a stereotactic body frame. *Int J Radiat Oncol Biol Phys* 2005;63:1427–31.
- [72] Shibamoto Y, Hashizume C, Baba F, et al. Stereotactic body radiotherapy using a radiobiology-based regimen for stage I nonsmall cell lung cancer: a multicenter study. *Cancer* 2012;118:2078–84.
- [73] Shirata Y, Jingu K, Koto M, et al. Prognostic factors for local control of stage I non-small cell lung cancer in stereotactic radiotherapy: a retrospective analysis. *Radiat Oncol* 2012;7:182.
- [74] Haasbeek CJ, Lagerwaard FJ, Antonisse ME, Slotman BJ, Senan S. Stage I nonsmall cell lung cancer in patients aged > or =75 years: outcomes after stereotactic radiotherapy. *Cancer* 2010;116:406–14.
- [75] Takeda A, Sanuki N, Kunieda E, et al. Stereotactic body radiotherapy for primary lung cancer at a dose of 50 Gy total in five fractions to the periphery of the planning target volume calculated using a superposition algorithm. *Int J Radiat Oncol Biol Phys* 2009;73:442–8.
- [76] Travis EL, Tucker SL. Isoeffect models and fractionated radiation therapy. *Int J Radiat Oncol Biol Phys* 1987;13:283–7.
- [77] Brenner DJ, Hlatky LR, Hahnfeldt PJ, Huang Y, Sachs RK. The linear-quadratic model and most other common radiobiological models result in similar predictions of time-dose relationships. *Radiat Res* 1998;150:83–91.
- [78] Withers HR, Thames Jr HD, Peters LJ. A new isoeffect curve for change in dose per fraction. *Radiother Oncol* 1983;1:187–91.
- [79] Sachs RK, Hahnfeldt P, Brenner DJ. The link between low-LET dose-response relations and the underlying kinetics of damage production/repair/misrepair. *Int J Radiat Biol* 1997;72:351–74.
- [80] Carlson DJ, Stewart RD, Semenenko VA, Sandison GA. Combined use of Monte Carlo DNA damage simulations and deterministic repair models to examine putative mechanisms of cell killing. *Radiat Res* 2008;169:447–59.
- [81] Keall P, Webb S. Optimum parameters in a model for tumour control probability, including interpatient heterogeneity: evaluation of the log-normal distribution. *Phys Med Biol* 2007;52:291.